Journal of Electronic Materials (2022) 51:6540–6546
https://doi.org/10.1007/s11664-022-09895-y

ORIGINAL RESEARCH ARTICLE

# Physicochemical Properties of Sodium Bis(2-methyllactato)borate Films Doped with Iodine for Photonic Applications

**Ahmad A. Ahmad[1] · Qais M. Al-Bataineh[1,2,3] · Areen A. Bani-Salameh[1] · Ahmad M. Alsaad[1] · Ahmad Telfah[2,4]**

Received: 15 April 2022 / Accepted: 19 August 2022 / Published online: 12 September 2022


## Abstract

In this work, semiorganic crystal films based on sodium bis(2-methyllactato)borate (NaMB) doped with iodine ($I_2$) were deposited on glass substrates using the dip-coating technique. The chemical, crystalline, and morphological structures were investigated. NaMB semiorganic crystal film has a monoclinic crystal structure with a P21/n space group and a crystallinity degree of 89.8%. Introducing $I_2$ into NaMB films reduces the crystallinity of the semiorganic crystal films. Moreover, the optical and electrical properties were investigated, including the refractive index, extinction coefficient, band structure, optoelectronic parameters, and electrical conductivity. Adding $I_2$ to NaMB films led to a decrease in the bandgap energy due to the formation of polarons between the valance and conduction bands. Finally, NaMB/$I_2$ semiorganic crystal film conductivity increases as the $I_2$ concentration increases, creating deep localized states in NaMB, leading to gap-state density changes by shifting the Fermi level and increasing the electrical conductivity.

**Keywords** Semiorganic crystal films · sodium bis(2-methyllactato) borate (NaMB) · iodine ($I_2$) · electronic transition band · electrical conductivity

## Introduction

In recent years, semiorganic crystal films have attracted increasing scientific research attention because of their interesting applications in photonic, optoelectronic, and sensor devices.[1–4] Semiorganic crystal films were developed due to their excellent optical and electrical properties and reliable physicochemical stability.[5,6] For instance, these films have high transparency, chemical flexibility, and thermal and mechanical stability.[7]

Research has focused on synthesizing semiorganic crystalline thin films grown using 2-methyllactic acid due to the presence of H-bonding to improve their optoelectronic and physicochemical properties.[8] Gokila et al.[8] synthesized bis(2-methyllactato)borate tetrahydrate to demonstrate the orthorhombic structure, which revealed fair crystallinity and transmission bandwidth between 220 nm and 1100 nm. Gokila et al.[9,10] then reported that sodium bis(2-methyllactato)borate (NaMB) hemihydrate has good crystallinity and excellent optical properties, making it a potential candidate for many optoelectronic applications due to its high transparency in the visible region.

The physical and chemical properties of complex composites grown based on NaMB hemihydrate doped with iodine ($I_2$) as novel materials were inspected to develop convenient films for optoelectronic applications. Iodine influences organic–halogen complexes, which affects their optical and dielectric properties.[11] The electrical conductivity of the semiorganic crystal films increases by incorporation of electron donors or acceptors.[12] Iodine ($I_2$) was chosen as the electron acceptor dopant in the polymers because of its significant influence on the optical, electrical, and dielectric properties.[13,14] Therefore, the physicochemical properties of the NaMB/$I_2$ semiorganic crystal films were investigated via their chemical, crystalline, morphological, and thermal properties. In addition, the optical and electrical properties

✉ Ahmad A. Ahmad
sema_just@yahoo.com

1 Department of Physical Sciences, Jordan University of Science & Technology, P.O. Box 3030, Irbid 22110, Jordan

2 Leibniz Institut für Analytische Wissenschaften-ISAS-e.V., Bunsen-Kirchhoff-Straße 11, 44139 Dortmund, Germany

3 Experimental Physics, TU Dortmund University, 44227 Dortmund, Germany

4 Hamdi Mango Centre for Scientific Research (HMCSR), the University of Jordan, Amman 11942, Jordan

of the NaMB/$I_2$ semiorganic crystal film were explored to investigate their feasibility in optoelectronic and photonic applications.

## Experimental Details

### Synthesis of Semiorganic Crystal Films Based on NaMB/$I_2$

NaMB thin films were fabricated by dissolving 4.164 g of 2-methyllactic acid ($C_4H_8O_3$, 104.11 g mol$^{-1}$, Sigma-Aldrich) in 100 mL deionized water using a magnetic stirrer, after which 1.236 boric acid ($H_3BO_3$, 61.83 g mol$^{-1}$, Sigma-Aldrich) was added to the 2-methyllactic acid solution. Finally, 1.050 g of sodium carbonate ($Na_2CO_3$, 105.99 g mol$^{-1}$, Sigma-Aldrich) was added to the mixed solution. The NaMB solution was homogenized using a magnetic stirrer for 2 h at room temperature. Then, NaMB/$I_2$ solutions with various weight percentages of $I_2$ (2.5, 5, 10 wt.%) were prepared by adding iodine ($I_2$, 253.8089 g mol$^{-1}$, Sigma-Aldrich) to the NaMB solution under continuous stirring at room temperature for 2 h. In addition, 1.0 g of polyvinylpyrrolidone (PVP) was added to the final solutions before deposition of the films to enhance their adhesion property. NaMB/$I_2$ films were prepared by immersing the glass substrates in the solutions for 2 h to produce one-layer semiorganic crystal films with 500 nm thickness.

### Characterizations of Semiorganic Crystal Films Based on NaMB Doped with $I_2$

A double-beam UV–Vis spectrophotometer (U-3900H) and four-point probe (Microworld) connected to a high-resolution multimeter (Keithley 2450 SourceMeter) were used to investigate the optical and electrical properties of the films. Fourier transform infrared spectrometry (FTIR) (Bruker Tensor 27 spectrometer) was used to investigate the chemical structural bonding by studying the vibrational bands. Moreover, the structural and morphological properties were investigated using x-ray diffraction analysis (XRD) (Malvern Panalytical Ltd) and scanning electron microscopy (SEM) (FEI Quanta 450 FEG).

## Results and Discussion

### Chemical Structure Analysis

The asymmetric unit of NaMB [$Na(C_8H_{12}BO_6)$] is composed of sodium cation and bis(2-methyllactato) borate

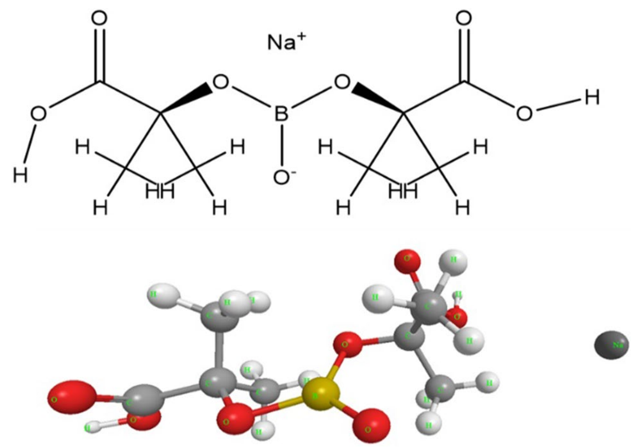

**Fig. 1** 2D and 3D molecular structure of NaMB crystal (data imported from reference).[9]

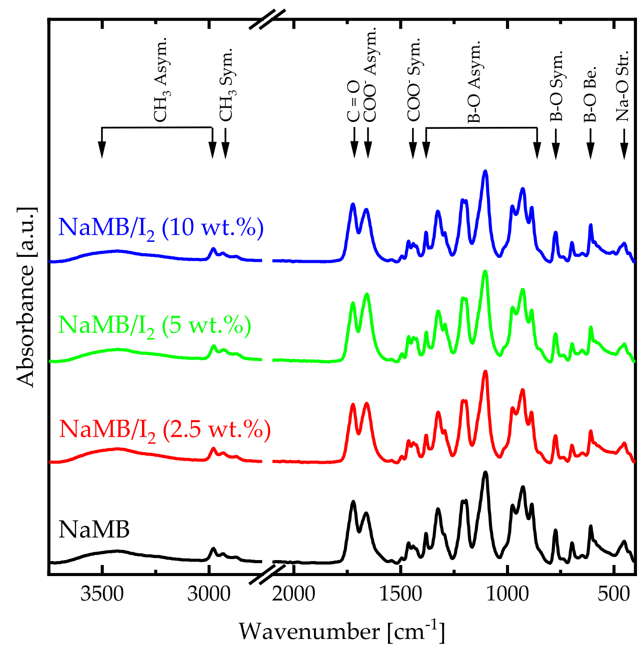


**Fig. 2** FTIR spectra of NaMB/$I_2$ semiorganic crystal films.

anion (Fig. 1). The NaMB film has infrared (IR) bands at 3400 cm, 2900 cm$^{-1}$ ($CH_3$ asymmetric stretching), 2930 cm$^{-1}$ ($CH_3$ symmetric stretching), 1720 cm$^{-1}$ (C=O stretching), 1655 cm$^{-1}$ ($COO^-$ asymmetric stretching), 1450 cm$^{-1}$ ($COO^-$ symmetric stretching), 1380–880 cm$^{-1}$ (B-O asymmetric stretching), 775 cm$^{-1}$ (B-O symmetric stretching), 610 cm$^{-1}$ (B-O bending), and 460 cm$^{-1}$ (Na-O stretching) (Fig. 2). Doping of NaMB films with $I_2$ changes the band line width and positions due to the difference in the electronegativity of iodine and the NaMB atoms.[14]

## Structural and Morphological Analysis

Structural analysis of the NaMB/$I_2$ semiorganic crystal film was performed using the powder XRD method (Fig. 3a). The indexing of the XRD peaks was investigated using Qualx2 qualitative phase analysis software. NaMB semiorganic crystal film has a monoclinic structure with a P21/n space group, with different diffraction peaks at Bragg's angles (Miller indices) 11.82° (011), 12.59° (110), 17.49° (002), 18.96° (120), 21.18° (210), 22.51° (121), 23.99° (022), 28.63° (122), 29.93° (300), 31.49° (032), 36.34° (041), and 38.43° (231). The XRD peaks agree well and match the standard monoclinic NaMB (JCPDS 00-155-0583). In addition, X'Pert HighScore Plus software was used to calculate the unit cell parameters (Table I), which also agree with the literature.[9,10] The degree of crystallinity of the NaMB semiorganic crystal films was evaluated using the equation: $X_{cryst} = 100\% \times A_{crys}/(A_{crys} + A_{Amp})$ and found to be 89.8%, indicating it has a highly crystal structure. Doping of NaMB with $I_2$ decreases the film's degree of crystallinity to 74.1% with an iodine weight percent of 10 wt.%. The reduction in the crystallinity orders upon iodine incorporation is attributed to the structural disruption of the NaMB due to its interaction with iodide ($I^-$), triiodide ($I^{3-}$), and the molecular iodine ($I_2$), which reduces the intermolecular interactions in the NaMB crystals. NaMB semiorganic crystal film demonstrates a crystal nature with a semi-smooth surface (Fig. 3b). Doping of NaMB film with $I_2$ (10 wt.%) decreases the crystal nature and increases the film's roughness (Fig. 3c).

Williamson–Hall method (WH) was used to calculate the crystallite size ($D$) and microstrain $\langle\varepsilon\rangle$ based on the following equation[15]:

$$\beta_{hkl}\cos\theta = \frac{k\lambda}{D} + 4\varepsilon\sin\theta \tag{1}$$

where $\beta_{hkl}$ is the diffraction peak line width (in radians), $\theta$ is the diffraction angle, and $k$ is the Scherrer constant and is equal to 0.9. A plot of ($4\sin\theta$) versus ($\beta_{hkl}\cos\theta$) in relevance to each diffraction peak reveals the crystallite size ($D$) and the microstrain $\langle\varepsilon\rangle$ (Table I). The crystallite size is similar to

**Table I** The crystal and thermal parameters of NaMB/$I_2$ semiorganic crystal films.

| Parameter | NaMB | NaMB/$I_2$ (2.5 wt.%) | NaMB/$I_2$ (5 wt.%) | NaMB/$I_2$ (10 wt.%) |
|---|---|---|---|---|
| a [Å] | 10.0 | 10.0 | 10.0 | 10.0 |
| b [Å] | 11.1 | 11.2 | 11.2 | 11.2 |
| c [Å] | 11.3 | 11.4 | 11.4 | 11.4 |
| β [°] | 116.1 | 116.1 | 116.1 | 116.1 |
| $\mathbf{X_{cryst}}$[%] | 89.8 | 83.3 | 81.8 | 74.1 |
| $\boldsymbol{D}$ [nm] | 16 | 16 | 16 | 16 |
| $\langle\varepsilon\rangle \times 10^{-3}$ | 2.2 | 3.1 | 6.7 | 9.4 |
| $\boldsymbol{T_m}$ [°C] | 71.2 | 72.6 | 78.4 | 82.7 |
| $\Delta\boldsymbol{H_m}$ [J/g] | 6.39 | 6.19 | 3.84 | 3.52 |

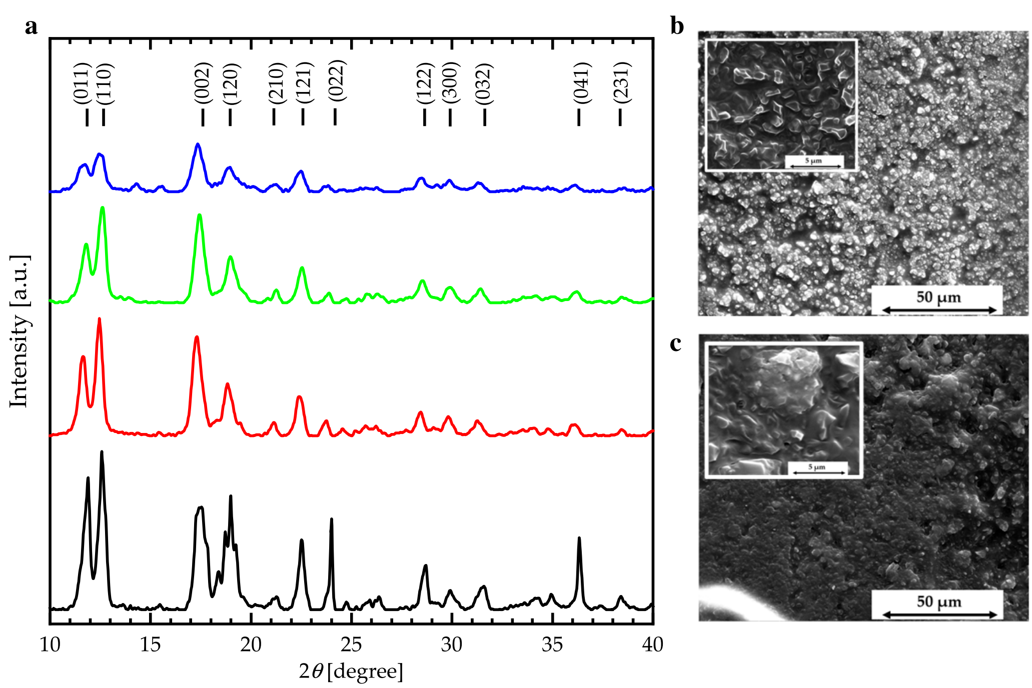


**Fig. 3** (a) XRD pattern of NaMB/$I_2$ semiorganic crystal films, (b) SEM micrograph of NaMB semiorganic crystal films, and (c) SEM micrograph of NaMB/$I_2$ (10 wt.%) semiorganic crystal films.

all NaMB/$I_2$ semiorganic crystal films (16 nm). The reason is that iodine interacts with sodium ions outside the host matrix and does not affect the crystallite size of the main composite. However, the microstrain value increases as $I_2$ concentration increases in the NaMB crystals, which is consistent with the crystallinity degree results.

## Differential Scanning Calorimetry (DSC)

Figure 4 shows the DSC curves of NaMB/$I_2$ semiorganic crystal films with different concentrations of $I_2$ -revealing endothermic peaks relevant to their melting temperatures ($T_m$). The DSC curve shows that the melting temperature of the pure NaMB was around 70°C with a melting enthalpy ($\Delta H_m$) of 6.39 J/g (Table I). Increasing $I_2$ in the NaMB films up to 10 wt.% increases the melting temperature until it reaches 83°C. In addition, the melting enthalpy ($\Delta H_m$) decreases continuously to 3.82 J/g as $I_2$ concentration increases to 10 wt.%.

## Optical Properties and Electronic Band Structure

The transmittance spectrum of NaMB semiorganic crystal film increases abruptly from 0 to 88% as the incident photon wavelength increases from 300 to 380 nm, with variations no longer occurring in the spectral range of 380–700 nm (Fig. 5a). The significant transmittance of the NaMB films is attributed to the lack of free electrons in the NaMB crystals. However, knocking out the crystal electrons in the valance band and transforming them into the conduction band requires high photon energy (UV light). The incorporating of $I_2$ into the NaMB crystal films leads to shifting of the absorption edge to the red region, consequently decreasing the bandgap energy due to the formation of polaron states between the valance and conduction bands. In addition, NaMB/$I_2$ semiorganic crystal film (10 wt.%) has lower transmittance than that of the other films due to the free photon-absorbing electrons in iodide ($I^-$) and triiodide ($I^{3-}$) ions with lower energies. NaMB semiorganic crystal films with the incorporation of $I_2$ have transmittance values of zero in the spectral range of 250–400 nm, which means that NaMB/$I_2$ semiorganic crystal films could be feasible as UV-light-shielding filters. The reflectance spectra exhibit a decreasing trend, with a broad drop in the spectral range of 300–500 nm (Fig. 5b), resulting from the formation of the polaron states between the valance and conduction bands of the NaMB composite.

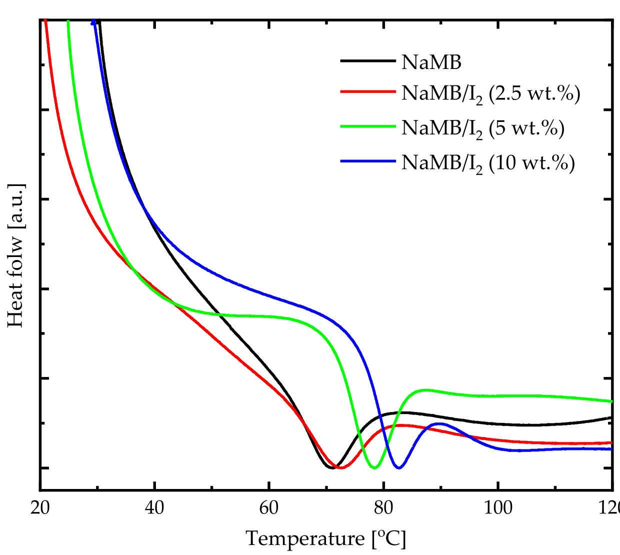


**Fig. 4** DSC curves of NaMB/$I_2$ semiorganic crystal films.

The extinction coefficient ($k$) was calculated by the equation $k = \alpha\lambda/4\pi$, where $\alpha$ is the absorption coefficient, given by $\alpha = (1/d)\ln((1 - R)/T)$.[16] The $k-$ spectrum for NaMB semiorganic crystal film has an absorption band at 280 nm due to the electron transition band between the valance and conduction bands (Fig. 5c). The low $k$-values of the NaMB semiorganic crystal film indicate that the photons pass through the film without any scattering or absorption. The $k$-spectra of the NaMB/$I_2$ semiorganic crystal films have two additional sub-bands at $I_2$ concentrations of 2.5 and 5 wt.% and three additional sub-bands at $I_2$ concentrations of 10 wt.% at 300, 360, and 420 nm, which represents the complex formation between NaMB and $I^-$, $I^{3-}$, and $I_2$ molecules (Fig. 6).[17] The dissolution of $I_2$ in the NaMB crystals can be described as[18]:

$$I_2 + 2e^- \leftrightarrow I^- + I^- \quad (2)$$

$$I^- + I_2 \leftrightarrow I_3^- \quad (3)$$

The refractive index ($n$) spectra were investigated based on the reflectance and extinction coefficient values using the equation $n = (1 + R/1 - R) + \sqrt{\left(4R/(1 - R)^2\right) - k^2}$.[16] The $n-$ spectrum of NaMB semiorganic crystal film decreases from 2.1 to 1.5 as the incident photon wavelength increases from 250 nm to 700 nm (Fig. 5d). The reflectance spectra exhibit a decreasing trend, with a vast drop in the spectral range of 300–500 nm, resulting from the formation of polaron states between the valance and conduction bands of NaMB.

The Tauc method was used to determine the optical bandgap energy of the NaMB/$I_2$ semiorganic crystal films by plotting $(\alpha h\nu)^2$ versus $h\nu$, according to the Tauc equation $(\alpha h\nu)^2 = \beta(h\nu - E_g)$.[19,20] In addition, the substates between the valance and conduction bands resulting from the disorder in the NaMB/$I_2$ semiorganic crystal films were investigated using the Urbach energy ($E_U$) via the equation $\alpha = \alpha_0 \exp(h\nu/E_U)$.[21] Increasing $I_2$ in the NaMB crystal decreased the $E_g$ value and increased the $E_U$

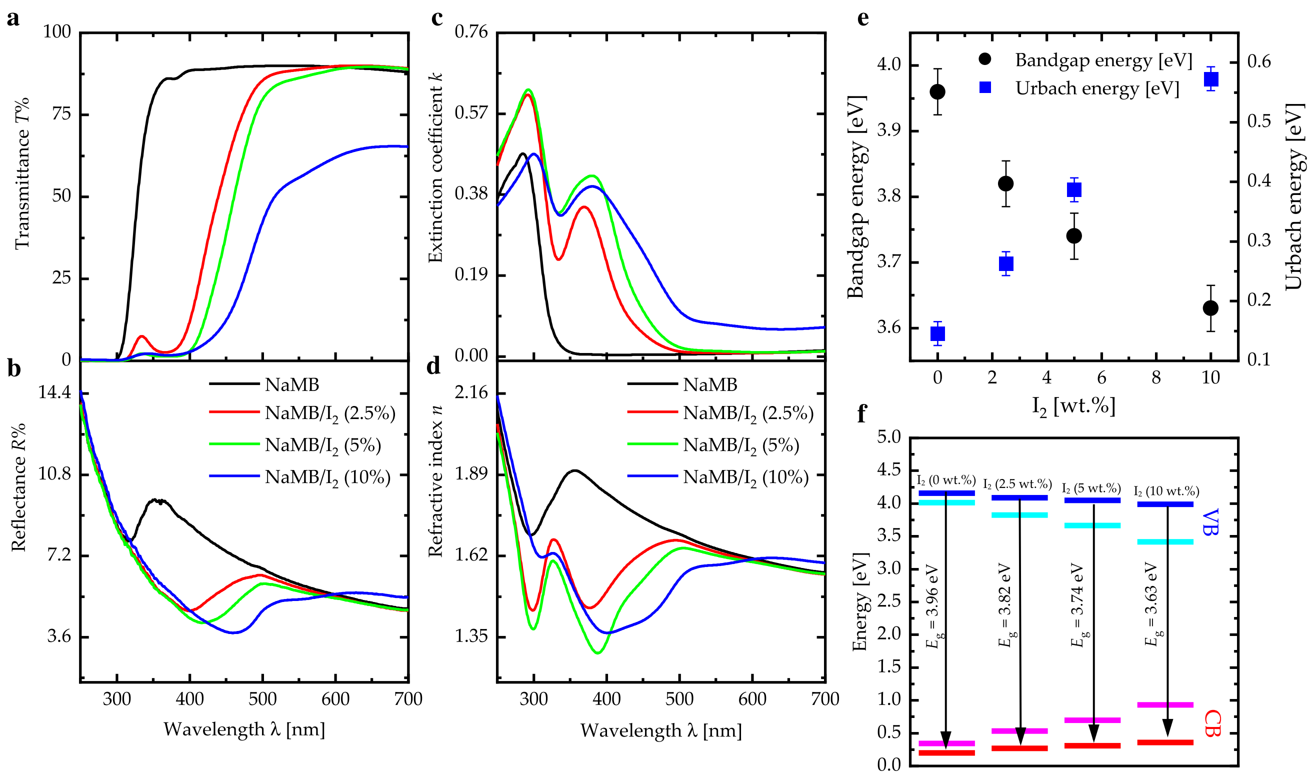


**Fig. 5** (a) Transmittance, (b) reflectance, (c) extinction coefficient, (d) refractive index spectra of NaMB/$I_2$ semiorganic crystal films, (e) optical bandgap energy and Urbach energy of NaMB/$I_2$ semiorganic crystal films as a function of $I_2$ concentration, and (f) schematic diagram of the band structure for NaMB/$I_2$ semiorganic crystal films.

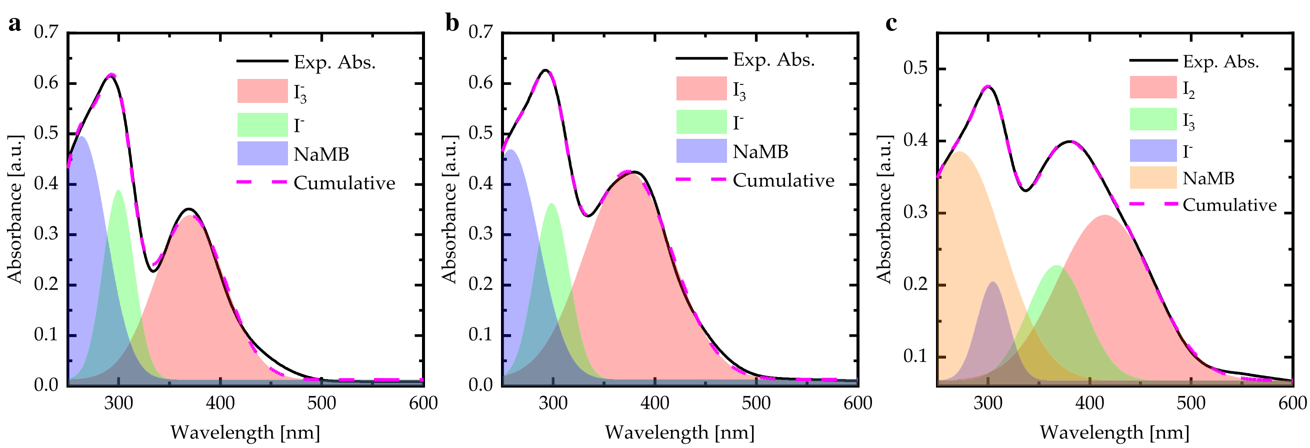


**Fig. 6** The multiple peaks fit NaMB/$I_2$ semiorganic crystal film's extinction coefficient spectra with $I_2$ concentrations of (a) 2.5 wt.%, (b) 5 wt.%, and (c) 10 wt.%.

value (Fig. 5e), which means that the NaMB exhibited cationic behavior, with the iodine anion forming polaron states between the valance and conduction bands, and consequently decreasing the bandgap energy.[22] In addition, the abrupt increase in the bandgap energy of the NaMB/$I_2$ semiorganic crystal film upon increasing the $I_2$ concentration changed the film behavior from dielectric to semiconducting. Based on the literature, the new band structure, including the $E_{VB}$, $E_{CB}$, optical bandgap energy, and the substates, were investigated using the ionization energy and the electron affinity energy.[23,24] Finally, the schematic diagram of the band structure for NaMB/$I_2$

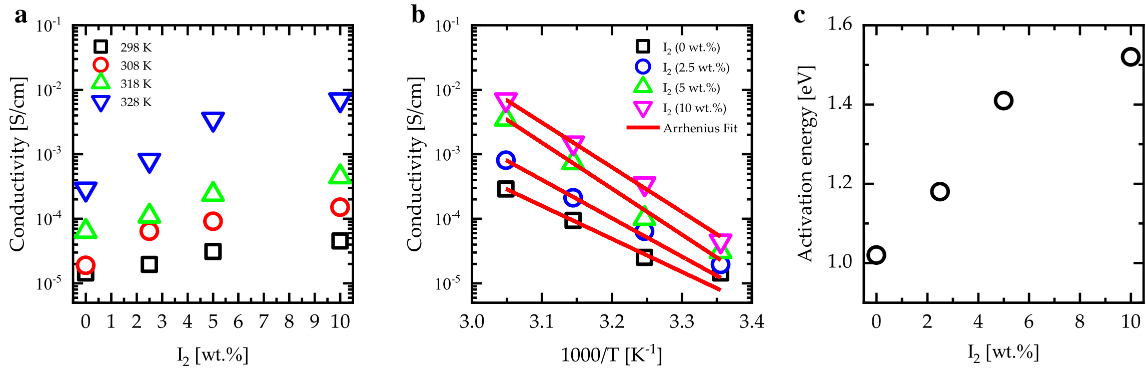


**Fig. 7** (a) The electrical conductivity of NaMB/$I_2$ semiorganic crystal films for different temperatures as a function of $I_2$ concentrations, (b) electrical conductivity of NaMB/$I_2$ semiorganic crystal films as a function of 1000/T [$K^{-1}$], and (c) activation energy deduced from conductivity fitted to the Arrhenius equation in the temperatures range of 298–328 K.

semiorganic crystal films showed a decrease in the $E_{VB}$ and an increase in the $E_{CB}$, which enhanced the decreasing trend in $E_g$ as the $I_2$ concentration increased (Fig. 5f).

## Electrical Conductivity

Figure 7a illustrates the electrical conductivity for the NaMB/$I_2$ semiorganic crystal films for different temperatures as a function of $I_2$ concentrations. The electrical conductivity of the NaMB/$I_2$ semiorganic crystal film increased from 0.14 to 0.45 μS/cm by increasing the $I_2$ concentration to 10 wt.%. The increase in the electrical conductivity values upon increasing $I_2$ concentration can be attributed to the creation of deep localized states in NaMB, which creates embedded gap states with densities changing by shifting the Fermi level and increasing the electrical conductivity.[24] Moreover, increasing the temperature increases the electrical conductivity (Fig. 7a) due to an increase in the cationic thermal activation, which causes a cation to jump to the following coordinating sites and increases the amorphous phase in the semiorganic films.[25] Figure 7b shows the variation in electrical conductivity ($\sigma$) as a function of temperature [1000/T(K)] for the NaMB/$I_2$ semiorganic crystal films for different $I_2$ wt.% fitted via the Arrhenius equation, which means that the samples are thermally activated. Arrhenius-like behavior for $\sigma$ can be defined as $\sigma = \sigma_0 \exp(-E_a/K_B T)$, where $\sigma_0$ is the pre-exponential factor, T is the temperature [K], $K_B$ is the Boltzmann constant, and $E_a$ is the activation energy.[26] The activation energy increases by introducing $I_2$ and enhances the electrical conductivity (Fig. 7c).

## Conclusions

The chemical, structural, morphological, optical, and electrical properties of NaMB/$I_2$ semiorganic crystal films with different weight percents of $I_2$ were investigated. FTIR spectra and XRD patterns of NaMB/$I_2$ semiorganic crystal films confirmed the charge transfer between $I_2$ and NaMB crystals. Based on the XRD measurements, NaMB polymer film has a monoclinic crystal structure with a P21/n space group and a degree of crystallinity of 89.8%. Increasing the $I_2$ content in the NaMB crystals decreased the crystallinity degree to 74.1% due to disruption of the structure of NaMB. This disruption occurs as a result of the interactions between the NaMB atoms and iodide ($I^-$), triiodide ($I^{3-}$), and the molecular iodine ($I_2$), which reduces the intermolecular interactions in the NaMB crystals. Moreover, introducing $I_2$ in NaMB crystals decreases the optical bandgap energy due to the formation of polaron states between the valance and conduction bands. The decrease in the bandgap leads to blocking of light in the wavelength range of 250–400 nm; consequently, NaMB/$I_2$ semiorganic crystal films are potential candidates for use as UV-light-shielding filters. The average electrical conductivity of the NaMB/$I_2$ semiorganic crystal film increased from 0.14 to 0.45 S/cm with the increase in the $I_2$ concentration to 10 wt.%. Adding $I_2$ to the composite led to deep localized states in NaMB, which changed the gap-state densities by shifting the Fermi level and increasing the electrical conductivity.

**Acknowledgments** The authors would like to acknowledge Jordan University of Science and Technology, the Deanship of Research, for the support in project number 016/2021. We also thank Prof. Mohammad-Ali H. Al-Akhras for helping our members use the biomedical laboratory. Thanks to Prof. Mohammad-Ali H. Al-Akhras for helping our members use biomedical laboratories.

**Author Contributions** A.A.A.: Conceptualization, Supervision, Methodology, Writing—review & editing. Q.M.A.-B.: Methodology, Writing—review & editing. A.A.B.-S.: Preparation, Data acquisition. A.M.A.: Data acquisition, Writing—review & editing. A.T.: Conceptualization, Writing—review & editing.

**Conflict of interest** The authors declare that they have no known competing financial interests or personal relationships that could have influenced the work reported in this paper.

**Consent to participate** All authors participated in this work.

**Consent to publish** All authors agree to publish this work.

## References

1. K.R. Mohan, V. Achari, V. Rao, and A. Sharma, Electrical and optical properties of (PEMA/PVC) polymer blend electrolyte doped with $NaClO_4$. *Polym. Test.* 30, 881–886 (2011).
2. S. Ibrahim, R. Ahmad, and M.R. Johan, Conductivity and optical studies of plasticized solid polymer electrolytes doped with carbon nanotube. *J. Lumin.* 132, 147–152 (2012).
3. H. Althues, J. Henle, and S. Kaskel, Functional inorganic nanofillers for transparent polymers. *Chem. Soc. Rev.* 36, 1454–1465 (2007).
4. C. Sanchez, B. Julián, P. Belleville, and M. Popall, Applications of hybrid organic–inorganic nanocomposites. *J. Mater. Chem.* 15, 3559–3592 (2005).
5. G. Gokila, R. Aarthi, and C.R. Raja, Structural, spectral and nonlinear optical analysis of Sodium bis (2-methyllactato) borate: a new semiorganic crystal for photonic applications. *Opt. Quant. Electron.* 52, 1–11 (2020).
6. G. Gokila, R. Aarthi, and C.R. Raja, Structural, Spectral, and Optical Characterization of Potassium bis (2-methyllactato) borate Hemihydrate Crystal. *J. Electron. Mater.* 49, 6130–6135 (2020).
7. B. Neelakantaprasad, G. Rajarajan, B. Ravi, and S. Masilamani, An investigation of optical constants, solid state parameters and NLO properties of glycine sodium iodide (GSI): a new auspicious semi organic NLO crystal for optoelectronics applications. *J. Mater. Sci.: Mater. Electron.* 29, 20225–20235 (2018).
8. G. Gokila, R. Aarthi, and R.C. Ramachandra, Structural, spectral and nonlinear optical analysis of Bis (2-methyllactato) borate tetrahydrate: a new nonlinear optical crystal for laser applications. *Optik* 207, 164384 (2020).
9. G. Gokila, A. Thiruvalluvar, and C. Ramachandra Raja, Sodium bis (2-methyllactato) borate. *IUCrData* 4, x190593 (2019).
10. G. Gokila, R. Aarthi, and C. Ramachandra Raja, Structural, spectral and nonlinear optical analysis of Sodium bis (2-methyllactato) borate: a new semiorganic crystal for photonic applications. *Opt. Quant. Electron.* 52, 1–11 (2020).
11. T.-H. Le, Y. Kim, and H. Yoon, Electrical and electrochemical properties of conducting polymers. *Polymers* 9, 150 (2017).
12. J.-L. Brédas, B. Thémans, J. Fripiat, J.-M. André, and R. Chance, Highly conducting polyparaphenylene, polypyrrole, and polythiophene chains: An ab initio study of the geometry and electronic-structure modifications upon doping. *Phys. Rev. B* 29, 6761 (1984).
13. S. Chand, and N. Kumar, Effect of iodine doping on electrical conduction in PVB films. *J. Mater. Sci. Lett.* 8, 1009–1010 (1989).
14. K. Bazaka and M.V. Jacob, Effects of iodine doping on optoelectronic and chemical properties of polyterpenol thin films. *Nanomaterials* 7, 11 (2017).
15. Q.M. Al-Bataineh, R. Ababneh, A. Bahti, A.A. Bani-Salameh, C.J. Tavares, and A. Telfah, Effect of hydrogen-related shallow donor on the physical and chemical properties of Ag-doped ZnO nanostructures. *J. Mater. Sci.: Mater. Electron.* 1, 1–12 (2022).
16. A. Ahmad, A. Alsaad, Q. Al-Bataineh, and M. Al-Naafa, Optical and structural investigations of dip-synthesized boron-doped ZnO-seeded platforms for ZnO nanostructures. *Appl. Phys. A* 124, 458 (2018).
17. A. Telfah, M.-A. Al-Akhras, K.A. Al-Izzy, A.A. Ahmad, R. Ababneh, M.J.A. Ahmad, C.J. Tavares, and R. Hergenröder, Dielectric relaxation, XPS and structural studies of polyethylene oxide/iodine complex composite films. *Polym. Bull.* 79, 3759–3778 (2022).
18. M. Telfah, A. Ahmad, A. Alsaad, Q.M. Al-Bataineh, and A. Telfah, Doping mechanism and optical properties of as-prepared polyvinyl chloride (PVC) doped by iodine thin films. *Polym. Bull.* 1, 1–20 (2022).
19. A.A. Ahmad, Q.M. Al-Bataineh, I.A. Aljarrah, and A.D. Telfah, Electrochemical degradation of methyl red in zinc hydroxide and zinc oxide thin films, physical and chemical activation. *Mater. Chem. Phys.* 280, 125793 (2022).
20. A.A. Ahmad, A.A. Bani-Salameh, and Q.M. Al-Bataineh, Optical, structural and morphological properties of synthesized PANI-CSA-PEO-based GaN nanocomposite films for optoelectronic applications. *Polym. Bull.* 1, 1–20 (2022).
21. P. Norouzzadeh, K. Mabhouti, M. Golzan, and R. Naderali, Investigation of structural, morphological and optical characteristics of Mn substituted Al-doped ZnO NPs: a Urbach energy and Kramers-Kronig study. *Optik* 204, 164227 (2020).
22. A.S. Hassanien and A.A. Akl, Effect of Se addition on optical and electrical properties of chalcogenide CdSSe thin films. *Superlattices Microstruct.* 89, 153–169 (2016).
23. Q.M. Al-Bataineh, A.A. Ahmad, A. Alsaad, and A.D. Telfah, Optical characterizations of PMMA/metal oxide nanoparticles thin films: bandgap engineering using a novel derived model. *Heliyon* 7, e05952 (2021).
24. V. Arkhipov, P. Heremans, E. Emelianova, G. Adriaenssens, and H. Bässler, Charge carrier mobility in doped disordered organic semiconductors. *J. Non-Cryst. Solids* 338, 603–606 (2004).
25. M. A. AL-Akhras, S. E. Alzoubi, A. A. Ahmad, R. Ababneh, and A. Telfah, Studies of composite films of polyethylene oxide doped with potassium hexachloroplatinate. *J. Appl. Polym. Sci.* 138, 49757 (2021).
26. A. Telfah, M.-A. Al-Akhras, K.A. Al-Izzy, A.A. Ahmad, R. Ababneh, M.J.A. Ahmad, C.J. Tavares, and R. Hergenröder, Dielectric relaxation, XPS and structural studies of polyethylene oxide/iodine complex composite films. *Polym. Bull.* 1, 1–20 (2021).